Available online at www.sciencedirect.com
SCIENCE DIRECT®
International Journal of Heat and Mass Transfer 48 (2005) 3921–3931
International Journal of HEAT and MASS TRANSFER
www.elsevier.com/locate/ijhmt

Heat transfer of rectangular narrow channel with two opposite scale-roughened walls

Shyy Woei Chang [a,*], Tong-Miin Liou [b], Ming Hsin Lu [c]

[a] Thermal Fluids Laboratory, Department of Marine Engineering, National Kaohsiung Marine University, No. 142, Haijhuan Road, Nanzih District, Kaohsiung 811, Taiwan, ROC
[b] Department of Power Mechanical Engineering, National Tsing Hua University, Hsinchu, Taiwan, ROC
[c] Department of Marine Engineering, National Kaohsiung Marine University, Taiwan, ROC

Received 30 December 2004; received in revised form 15 April 2005

Abstract

An experimental study of heat transfer and pressure drop in a rectangular channel roughened by scaled surfaces on two opposite walls with flows directed in the forward and downward directions for Reynolds numbers (Re) in the range of $1500 \leqslant Re \leqslant 15{,}000$ was performed. Nusselt number ratios between the scale-roughened and smooth-walled ducted flows (Nu/Nu_∞) were in the range of 7.4–9.2 and 6.2–7.4 for laminar forward and downward flows respectively. The Nu/Nu_∞ values for turbulent developed flows in the scale-roughened channel with forward and downward flows were about 4.5 and 3 respectively. A comparison of present data with reported results using different types of surface roughness demonstrated the better thermal performances of present scale-roughened channel with forward flow at conditions of $Re > 10{,}000$. Experimental correlations of heat transfer and friction coefficient were derived for the present scale-roughened rectangular channel.

Keywords: Scale roughness; Heat transfer augmentation

1. Introduction

A variety of passive techniques for heat transfer augmentation has been developed in order to cope with the ever mounting cooling duty of a heat transfer device. Enhanced surfaces for forced convection channel-flow are produced in many configurations ranging from protruding ribs [1–6], dimpled surfaces [7,8] to vortex generators [9,10]. The secondary fluid motions induced by the various types of surface ribs, such as transverse, angled, V-shaped and broken ribs produce complex three-dimensional flow fields. The enhancement of heat transfer in a channel roughened by inclined ribs is due to the penetration of protruding ribs across the boundary layers that causes the redevelopment of boundary layers, the turbulence promotion and the creation of large secondary vortex structures. The geometric parameters governing the flow characteristics in a rib-roughened channel involve the channel aspect ratio, rib blockage ratio, rib angle of attack, rib pitch-to-height ratio, rib aspect ratio and the manner of rib arrangement on two opposite walls such as in-line, staggered, crisscross and discrete. Heat transfer augmentation for this class of

* Corresponding author. Tel.: +886 7 8100888/5216; fax: +886 7 5721035.
E-mail address: swchang@mail.nkmu.edu.tw (S.W. Chang).

0017-9310/$ - see front matter © 2005 Elsevier Ltd. All rights reserved.
doi:10.1016/j.ijheatmasstransfer.2005.04.015

flow is about 2–3.5 times of smooth-walled channel level. The flow structure produced by dimpled surface is characterized by vortical fluid and vortex pairs those periodically shed from each dimple. A large up-wash region and packets of fluid emanating from the central regions of each dimple, accompanying with the periodically vortex shedding process, develop in the region near the dimple diagonals. This complex three-dimensional unsteady process results in the effective heat transfer enhancements over the flat parts of the dimpled surface. But the heat transfer elevation in the concave dimpled surface is less effective. It is noticed that here is no protruding element over the concave dimpled surface. Therefore, unlike the secondary flows in a rectangular channel with two opposite walls roughened by angled ribs, the one-, two- or four-cell vortical flows could not be generated over the cross-section of a dimpled channel. The absence of cross-plane large secondary vortex structures could prohibit the further heat transfer augmentation in a dimpled channel so that the spatially averaged Nusselt numbers over a dimpled surface are in the range of 1.85–2.89 times of the baseline Nusselt number in smooth-walled channel [7]. Another surface roughness that provides considerable heat transfer elevation employs the wing-type longitudinal vortex generator. Longitudinal vorticies are generated along the side edges of each vortex generator (VG) by separation of flow due to the pressure difference between the upstream and downstream side of VG. These VG-induced vortices swirl the main flow to enhance the fluid mixing close to and far from the wall that results in the considerable heat transfer augmentation [9]. However, due to the large cost of flow loss in VG channel, the two opposite walls fitted with VGs remains impractical on account of flow losses. An alternative approach by fitting VGs on one wall and rib-roughened surface on the opposite wall for heat transfer augmentation has been numerically examined [10]. The ratios of Nusselt number and friction coefficient between VG enhanced surface and smooth-walled channel were approximated in the ranges of 2.9–3.41 and 22.5–32 respectively for airflow with Reynolds numbers ranging from 25,000 to 150,000 [10]. In many applications such as the tail-end cooling of gas turbine blade and automotive heat exchangers, where the channel width-to-height ratio approaches 8:1, the transverse velocity induced by the angled ribs over the cross-section of narrow channel becomes relatively low compared with the mainstream velocity [11]. In the rectangular channels with width-to-height ratios of 1/4, 1/2, 1, 2 and 4, the pressure drop increments are about 8–16 times greater for the channel with width-to-height ratio of 4 if the same level of heat transfer augmentation is to be achieved [5]. Thus the thermal performance of rib-roughened channel, compared with the constant pumping power, decreases with the increase of channel width-to-height ratio [1–10]. Although a large store of information for heat transfer augmentation in rib-roughened channels has been recorded in the last decade, only relatively few studies attempt the channels with width-to-height ratios in the range of 8–10 [3,8,11,12]. For cooling applications of electronic chipsets with intensified circuit densities in a Notebook PC, which are strictly confined by the available machine height, the narrow channel becomes one remained option for heat sink design. However, justified by the reported values of heat transfer augmentation and thermal performance in the narrow channels from Sunden group [3,8,11], the higher levels of heat transfer augmentation and thermal performance factor are requested for cooling of gas turbine blade and CPU in a Notebook PC. This need urges the development of new enhanced surface using the scaled roughness arranged in the staggered manner. No previously published work is available to examine the heat transfer performance in the channel with two opposite walls roughened by scaled surfaces. In this respect, the absence of research efforts and the possibility of wide industrial applications that require strong stiffness for structure integrity have motivated the present study.

2. Experimental details

2.1. Apparatus

The experimental apparatus is shown in Fig. 1. The schematics of test assembly depicts in Fig. 1a. The test fluid, pressurized air, was fed from the IWATA SC 175C screw-type compressor unit (1) which was dehumidified and cooled to the ambient temperature through a refrigerating unit (2). The dry and cooled airflow was channeled through a set of pressure regulator and filter (3) with the mass flow rate to be metered and adjusted by the Tokyo Keiso TF-1120 mass flow meter (4) and the needle valve (5) respectively. The scale of present mass flow meter was 0.01 kg/h that incurred the maximum uncertainty for mass flow measurement of about 0.257%. A digital-display pressure transducer (6) measured the pressure level of coolant flow. Prior to entering the test channel with two opposite walls roughened by scales (7), the metered airflow was directed through a smooth-walled $150\ \text{mm} \times 100\ \text{mm} \times 15\ \text{mm}$ flow-calming section (8). The ratio of cross-sectioned area between test channel and flow-calming section was 1.875, which simulated the abrupt flow entry condition. Dimensions of test channel were $155\ \text{mm} \times 80\ \text{mm} \times 10\ \text{mm}$ which gives a channel aspect ratio of 8 and the hydraulic diameter of 17.8 mm. The flow-calming section was constructed by Teflon plates. A K-type thermocouple penetrated into the core of flow-calming section adjacent to the entrance of scale-roughened test channel that measured the coolant entry temperature. The flow entry

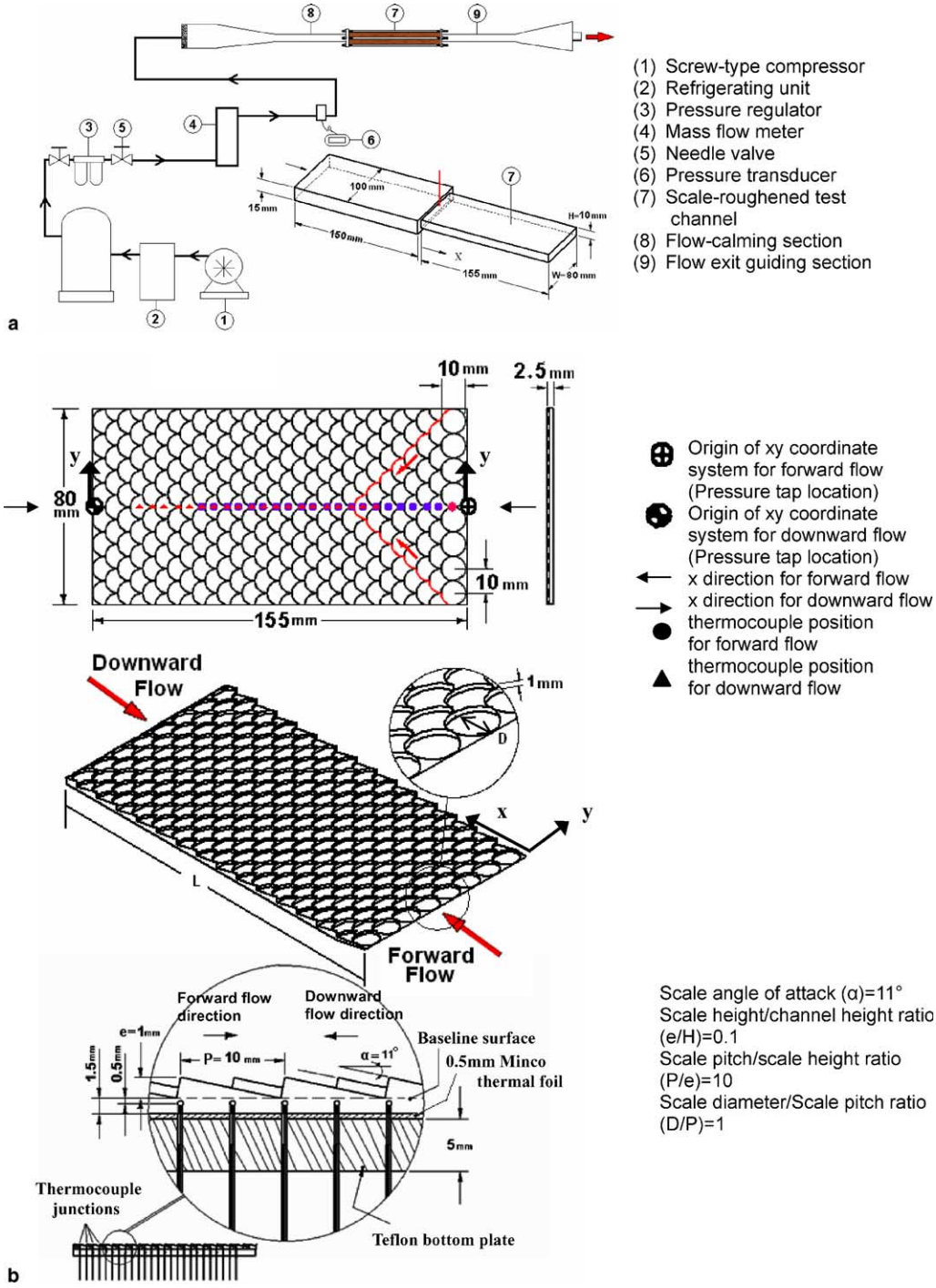

Fig. 1. Experimental facility: (a) experimental apparatus and (b) geometrical details of scale-roughened surface.

temperature was treated as the fluid reference temperature to define the fluid properties at the flow entrance, such as the specific heat, thermal conductivity and viscosity of coolant, for the evaluation of Reynolds and Prandtl numbers at flow entrance. The increment of flow bulk temperature from one measured station to its successive downstream station was determined using the sequential energy balance method. This sequential

energy accountancy calculated the flow bulk temperatures at the measured stations along the centerline of scale-roughened surface. At the exit-end of scale-roughened channel, three type K thermocouples, positioned with equal spanwise interval, penetrated into the core of exit guiding section (9) to measure the flow exit temperature. The flow exit temperature was used to check for the accuracy of energy accountancy based on the enthalpy balance method. Data batch was collected when the differences between the measured and calculated flow bulk temperatures were less than 10% at the exit plane.

Fig. 1b shows the geometrical details of the scale-roughened surface. Each two rows of scales in the artificially roughened surface were arranged in the staggered manner. The two opposite scale-roughened walls were in-line arrangement. The geometry of scaled surface was specified in terms of four non-dimensional parameters defined in Fig. 1b of

scale angle of attack (α) = 11°,
scale height/channel height ratio (e/H) = 1 mm/10 mm = 0.1,
scale pitch/scale height ratio (P/e) = 10 mm/1 mm = 10,
scale diameter/scale pitch ratio (D/P) = 10 mm/10 mm = 1.

The two opposite scale-roughened surfaces were electrically heated by two 0.5 mm thick Minco thermal foils sandwiched between Teflon bottom plate and scale-roughened surface which generated the basically uniform heat flux thermal condition. As pointed in Fig. 1b, K-type thermocouples with equal interval along the centerline of a scale-roughened surface were installed on the back face of the scale-roughened surface for wall-temperature measurements. All the temperature measurements were monitored and stored in a Dell PC using a Net-Daq Fluke Hydra 2640A data logger for the subsequent data processing. The wall-temperature measurement at each axial station was corrected into the base-line surface as indicated in Fig. 1b using the one-dimensional heat conduction law. The origins of coordinate systems for the forward and downward flows, which involved the streamwise (x) and spanwise (y) coordinates, were selected at the middle span of two side entry edges. It is worth mentioning that the wall-temperature variations over the scale-roughened surface were affected by the flow fields in the test channel. As the external-heat loss at each location over the roughened surface increased with the increase of wall-to-ambient temperature difference, the heat flux over the heating foil was not perfectly uniform even if the heat flux was uniformly generated by Minco heating foil. The distribution of convective heat flux was obtained by subtracting the local heat loss from the total heat flux supplied. Based on the results of heat-loss calibrations, the external-heat loss increased linearly with wall-to-ambient temperature difference. The local heat loss was estimated by multiplying the local wall-to-ambient temperature difference to the heat loss coefficient acquired from the heat loss calibrations. A review of the entire data of convective heat flux showed that the maximum non-uniformity in heat flux distribution was about 10.1%. The basically uniform heat flux heating condition was simulated by the present study.

The pressure drop and heat transfer tests were performed separately. Air was used as the test fluids in both tests and the pressure drop tests were conducted at isothermal conditions. To measure the pressure drop across the scale-roughened narrow channel, two tubes were equipped with pressure taps of 0.5 mm diameter at the two origins of coordinate systems as indicated in Fig. 1b. A short 1 mm diameter stainless steel tube was glued on top of each pressure tapping as connection for flexible tube. The pressure difference between two taps was measured with a Rosemount digital type micromanometer. The precision of this micromanometer was 0.001 mm-H_2O which provided the maximum uncertainty about 0.062% for this series of tests. This arrangement for pressure drop measurements included the flow resistance in the developing flow region. As the majority of flow region in the present scale-roughened channel for CPU cooling applications was under developing, this setup for pressure measurement provided an overall indication of the flow resistance in the entire scale-roughened channel, which measurement was higher than the developed flow value.

2.2. Program and data processing

Heat transfer and pressure drop tests over the scale-roughened surface were performed with the flows directed in the forward and downward directions at Reynolds numbers (Re) of 1500, 2000, 3000, 5000, 7500, 10,000, 12,500 and 15,000. This selected Re range covered the laminar and turbulent flows. The streamwise heat transfer distributions along the scale-roughened centerline and pressure drops across the test channel at various Reynolds numbers were examined. The manner by which the flow direction and Re affected the local and spatially averaged heat transfers and pressure drops was analyzed. A comparison of heat transfer and friction augmentations between the data collected from a variety of enhanced channels [1–8] and the present scale-roughened channel was performed to unravel the thermal performance of scale-roughened surface in narrow channel. Heat transfer and friction correlations were subsequently derived for forward and downward flows in the present scale-roughened channel that permitted the determination of local and spatially averaged Nusselt numbers and friction factors over scale-roughened surface for design application.

Steady state heat transfer measurements were performed at each set of predefined Reynolds number. The steady state was assumed when the variations of local wall temperatures with several successive scans were less than 0.3 °C. Depending on the heating level and flow condition, the elapsed time to achieve the steady state was about 30 min. Having satisfied the steady state assumption, the energy accountancy was checked to ensure the energy balance between the enthalpy increase of flow and the convective heat flux transferred to the bulk flow. It is noted that the various heat fluxes fed into the heating foil could also affect the Reynolds number even if the total amount of coolant mass flow rate remained invariant due to the thermal impact on fluids properties. Therefore, by adequately adjusting the coolant mass flow rate to compensate the varied fluid properties, the maximum variation in Reynolds number at the entry plane of test channel was controlled with ±1% for each targeting value.

For each acceptable data batch, the measurements of wall-temperature, coolant mass flow rate and heating power were collected for postdata processing. The Reynolds number, Re, and local Nusselt number, Nu, were evaluated using Eqs. (1) and (2) respectively.

$$Re = \rho W_m d/\mu \tag{1}$$

$$Nu = qd/[k_f(T_w - T_f)] \tag{2}$$

The symbols of ρ, W_m, d and μ in Eq. (1) respectively stand for the fluid density, bulk mean flow velocity, hydraulic diameter of test channel and viscosity of fluid. In Eq. (2), the convective heat flux, q, was obtained by subtracting the external-heat loss from the electrical dissipation measured over the heating surface. It is worth noting that the heating surface adopted for heat-flux evaluation included all profiles of the scaled surface. Having determined the local convective heat flux, the local Nusselt number, Nu, was subsequently defined using Eq. (1) in which T_w and T_f quoted for the wall and flow bulk temperatures respectively. All the fluid properties appeared in Eqs. (1) and (2) were evaluated from the local flow bulk temperature, T_f.

The Fanning friction factor, f, was calculated from the pressure drop, ΔP, across the test channel with length of L and the mean flow velocity as

$$f = \Delta P/(0.5\rho W_m^2)(d/4L) \tag{3}$$

The maximum uncertainty of temperature measurement for the present test conditions was ±0.3 °C, which was the major source to attribute the uncertainties of coolant's thermal conductivity, fluid density and viscosity. The maximum uncertainty associated with the local Nusselt and Reynolds numbers and the friction factor were estimated to be 11.7% and 4.6% and 2.3% respectively using the policy of ASME on reporting the uncertainties in experimental measurements and results [13].

To unravel the heat transfer augmentation and the friction-loss increase in the present test channel, the comparative references of heat transfer and friction factor were selected as the levels in smooth circular tube with fully developed flow. The reference Nusselt number, Nu_∞, and friction factor, f_∞, for laminar and turbulent flows were defined as

$$Nu_\infty = 48/11 \text{ (laminar flow)} \tag{4}$$

$$f_\infty = 16/Re \text{ (laminar flow)} \tag{5}$$

$$Nu_\infty = 0.023Re^{0.8}Pr^{0.4}$$
(Dittus–Boelter correlation for turbulent flow) (6)

$$f_\infty = 0.079Re^{-0.25}$$
(Blasius equation for turbulent flow) (7)

The thermal performance of the scale-roughened surface in the preset narrow channel was quantified by the performance factor, η, which was obtained by considering both the heat transfer augmentation and the friction-loss increase based on the constant pumping power condition. This performance factor is expressed as the following equation:

$$\eta = (Nu/Nu_\infty)/(f/f_\infty)^{\frac{1}{3}} \tag{8}$$

3. Results and discussion

3.1. Heat transfer

The streamwise heat transfer distributions along the centerline of scale-roughened surface at all the tested Reynolds numbers with forward and downward flows are presented in Fig. 2. For each Reynolds number tested, the local Nusselt numbers decay exponentially in the streamwise direction to approach a fully developed value. Justified by all the streamwise heat transfer variations shown in Fig. 2, the sharp entrance in the scale-roughened channel generates the developing flows in the spatial regions about $0 < x/d < 4.5$ and $0 < x/d < 5.5$ for forward and downward flows respectively. The appreciable streamwise zig-zag Nu variations only emerge in the developing flow region with the higher Nu value indicated at the middle point of two successive edges for each scale-pair. Unlike the downward flow scenario, the forward flow initially encounters the protruding circular edge of each scale so that the near-wall flow is confined to travel along the circular confront in each scale. After the flow traversing the protruding circular-edge further downstream, a declined face in downhill direction is followed to guide the streamwise flow until the successive protruding circular edge is encountered. As the present scales are arranged in the staggered manner, these protruding circular edges are conjoint to form

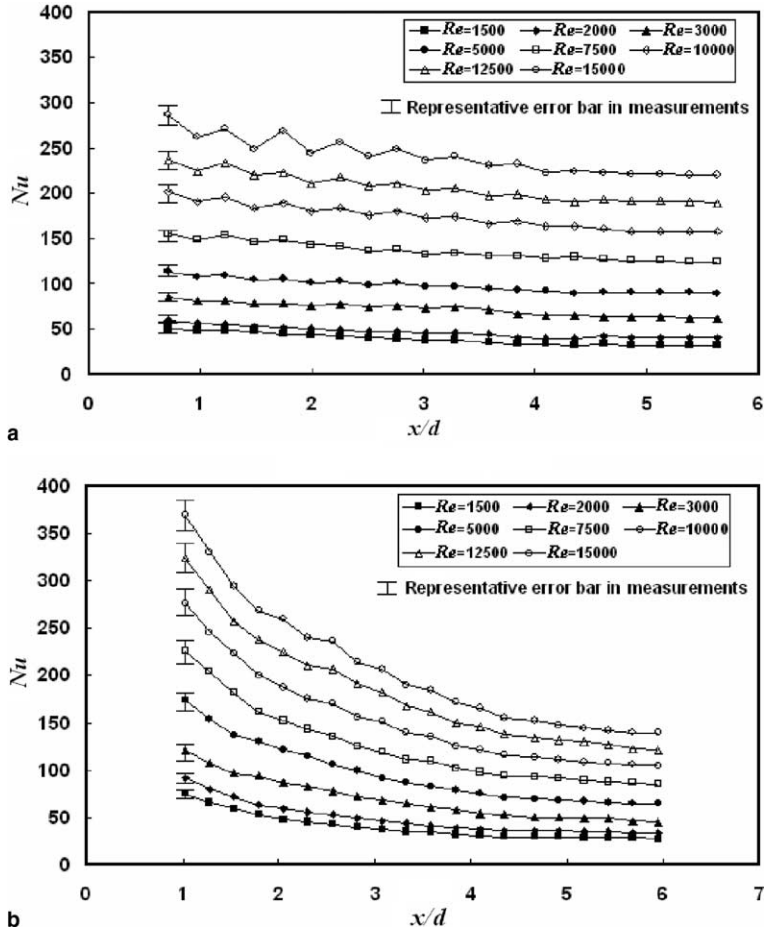

Fig. 2. Axial distributions of Nusselt number for forward and downward flows in scale-roughened channel: (a) forward flow and (b) downward flow.

a network of step-by-step V-shaped edges pointing downstream. The cross-plane secondary flow cells could accordingly be generated by two opposite scale-roughened surfaces that improve the fluid mixing. For downward flow condition, the coolant-stream flows over the scale-shaped cavities. The inclined surface behind each scale-edge is in the uphill direction rather than the downhill direction for forward flow. The network of step-by-step V-shaped edges, constructed by the edges of scales, is pointing upstream when the flow is directed downward. Therefore, the subtle differences in flow structures between the forward and downward flows in the present scale-roughened channel exist. Referring to the various rib-roughened and dimpled channels, the discontinued circular edges over each scale-roughened surface could similarly generate the spatial heat transfer variations. As the forward-flow traverses the protruding edges rather than flowing over the scale-edged cavities, the higher degree of zig-zag variation develops in the channel with forward flow. Such zig-zag *Nu* variations are amplified by increasing Reynolds number but gradually faded in the further downstream.

The complex flow structures generated in the scale-roughened channel could yield the functional relationship between *Nu* and *Re* from $Nu \propto Re^{0.8}$ [14]. The present heat transfer results at each axial station for all Reynolds numbers tested are well correlated by $Re^{0.815}$ and $Re^{0.7}$ for forward and downward flows respectively. As the streamwise distributions of local Nusselt number along the centerline of scale-roughened channel follow a simple exponential decay along the axis of channel towards the developed value, the experimental correlations, having the slight variation in *Pr* with maximum variation range of 1.68% been absorbed into the numerical coefficients of equations, are derived as

$$Nu = (0.0896 + 0.0596e^{-0.92\times(x/d)}) \times Re^{0.815} \quad \text{(for forward flow)} \tag{9}$$

$$Nu = (0.169 + 0.638e^{-0.81\times(x/d)}) \times Re^{0.7} \quad \text{(for downward flow)} \tag{10}$$

Over the entire range of Reynolds number studied, 91% of the present experimental Nusselt numbers are found to agree within ±10% variances with Eqs. (9) and (10). It is worth noting that the power indices of the exponential function appearing in Eqs. (9) and (10) are −0.92 and −0.81 respectively. In other words, the flows evolve into developed region after about 4.35 and 4.94 hydraulic diameters for forward and downward flows respectively. Nevertheless, since the Prandtl number effects are absorbed into the coefficients of equations (9) and (10) and are not included as a parameter in these correlations developed, the results of this study are essentially limited to dry air.

The attempt to identify the heat transfer enhancement in this scale-roughened channel is performed by comparing the Nusselt number data in developed flow region between the scale-roughened channel and smooth-walled tube in terms of $\overline{Nu}/Nu_\infty$. The Nusselt number value of developed flow in the present scale-roughened channel, $\overline{Nu}$, is obtained by averaging the local Nu data acquired from the developed flow region. When Re increases from 1500 to 15,000 as shown in Fig. 3, two different data trends with increasing and decreasing $\overline{Nu}/Nu_\infty$ ratios for both forward and downward flows develop at the Reynolds number between 2000 and 3000. This indicates that the flow transition from laminar to turbulent flows could take place at the Reynolds number between 2000 and 3000 for the present specific geometry. As shown in Fig. 3, the ratios of $\overline{Nu}/Nu_\infty$ for laminar flow with $Re < 3000$ increase with increased Re for both forward and downward flows in the present test channel. Heat transfer enhancement ratios in the scale-roughened channel with forward and downward laminar flows are respectively in the range of 7.4–9.2 and 6.2–7.4 times of smooth-walled tube level. In the developed turbulent flow region for the present Reynolds numbers examined, the heat transfer

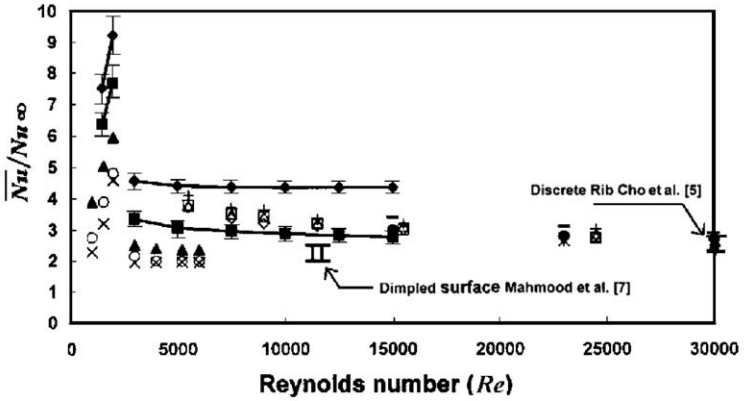

Symbols	References	Channel aspect ratio	Rib attack angle	P/e	e/H	Type of roughness
◆	Forward flow (present study)	8		10	0.1	Scaled surface
■	Downward flow (present study)	8		10	0.1	Scaled surface
◇	Taslim et al. 45deg V-Up [1]	1	45	10	0.083	Continuous rib
+	Taslim et al. 45deg V-Down [1]	1	45	10	0.083	Continuous rib
□	Taslim et al. 45deg [1]	1	45	10	0.083	Continuous rib
△	Taslim et al. V Discrete [1]	1	45	10	0.083	Discrete rib
●	Han et al. 45deg V-Up [2]	1	45	10	0.0625	Continuous rib
–	Han et al. 45deg V-Down [2]	1	45	10	0.0625	Continuous rib
✱	Han et al. 45deg [2]	1	45	10	0.0625	Continuous rib
×	Gao & Sunden 60deg V-Up [3]	8	60	10	0.1	Continuous rib
▲	Gao & Sunden 60deg V-Down [3]	8	60	10	0.1	Continuous rib
○	Gao & Sunden 60deg [3]	8	60	10	0.1	Continuous rib
▼	Park et al. 45deg Parallel [4]	4	45	10	0.125	Continuous rib
I	Cho et al. [5]	2	45	10	0.1	Discrete rib
II	Mahmood et al. [7]	16		8	0.4	Dimpled surface

Fig. 3. Comparison of Nusselt number ratios between scaled-roughened, dimpled and rib-roughened channels at various Reynolds numbers.

augmentations in terms of Nusselt number ratios respectively increase and decrease with increasing Reynolds number in the scale-roughened channels with forward and downward flows. As the scale-roughened surface provides a number of circular-shaped protruding edges to traverse flow, the flow could circulate among these scales with the vorticity enhanced. Also the protruding scales with inclined face could act as the discrete ribs in channel flow that periodically break the boundary layers to incur the spatial redevelopment of boundary layer. These near-wall flow mechanisms along with the enhanced vorticity improve the fluid mixing that attributes to heat transfer augmentation. Nevertheless, the variation manners of $\overline{Nu}/Nu_\infty$ against Re for turbulent flows as shown in Fig. 3 are due to the different power indices of Re for forward and downward flows in Eqs. (9) and (10), which are respectively 0.815 and 0.7. In this respect, the heat transfer enhancements provided by the scale-roughened surface with forward flow are not moderated at high Reynolds numbers, which offers a creditable characteristic among the surface-enhanced channels [1–11]. As compared in Fig. 3 with the heat transfer results reported by different research groups for rib-roughened channels [1–4], the present scale-roughened channel with forward flow appears to be the only scenario that shows the increased $\overline{Nu}/Nu_\infty$ with increased Re. Also the heat transfer improvement ratio of about 4.5 in the scale-roughened channel with forward flow is the highest value among the comparative groups [1–4]. However, in the scaled-roughened channel with downward flow, the value of $\overline{Nu}/Nu_\infty$ is about 3 which is similar to the square-sectioned channels roughened by 45° angled ribs [1,2]. It is worth mentioning that the heat transfer augmentations attributed to V-shaped ribs in narrow channel with width-to-height ratio of 8 [3] are less effective than those in square-sectioned channels [1,2] as compared in Fig. 3. In this respect, Park et al. [4] previously reported that the heat transfer augmentation provided by a variety of angled ribs decreased with the increase of channel width-to-height ratio. Due to the considerable very narrow rectangular channel with width-to-height ratio of 8 [11], the transverse velocity normal to the rib-roughened wall is not high so that the strength of flow cells generated over the sectioned plane of rib-roughened channel is relatively weak in comparison with the rib-roughened square channels. Further research aimed at examining the impact of channel aspect ratio on heat transfer in scale-roughened channel is worthwhile for the other industrial applications from the narrow channel flows.

3.2. Friction factor

Fig. 4 depicts the Reynolds number dependence of Fanning friction factor, f, which is calculated from the pressure drop across the entire test channel, for forward and downward flows. Two distinct variation manners of f versus Re for laminar and turbulent flows are found in Fig. 4a. In the range of $3000 \leqslant Re \leqslant 15{,}000$, the Fanning frictions factors in the present scale-roughened channel with forward and downward flows are respectively correlated as

$$f = 2.679 \times Re^{-0.318} \text{ (for forward flow)} \tag{11}$$

$$f = 8.836 \times Re^{-0.39} \text{ (for downward flow)} \tag{12}$$

The Fanning friction factors for forward and downward flows in the laminar and turbulent flow regimes decrease with increasing Reynolds number as depicted in Fig. 4a. The downward flow in the present scale-roughened channel consistently generates the higher friction factors than the forward-flow counterparts in the Re range of $1500 \leqslant Re \leqslant 15{,}000$. In order to unravel the friction augmentation from the smooth-walled tube levels due to the present scale-roughened surface, the plot of f/f_∞ against Re for forward and downward flows is shown in Fig. 4b. Also compared in Fig. 4b are the f/f_∞ data reported for the rib-roughened channels [1–6,8]. When the Reynolds number gradually increases, the friction ratios respectively decrease and increase for the scale-roughened and rib-roughened channels [1–4,6] as shown in Fig. 4a. The friction ratios in both scale-roughened and rib-roughened channels tend to approach the asymptotic values as the Reynolds number is further increased from 10,000. It is noticed that the magnitudes of friction augmentation in the present scale-roughened channel are higher than those in the rib-roughened channels. The effective heat transfer augmentation with $\overline{Nu}/Nu_\infty$ ratios in the range of 3–4.5 for the present scale-roughened channel is accompanying with the high pressure drop loss. From the application point of view, the pressure drop in the scale-roughened channel with forward flow has to be compensated if the high heat-flux transmissions with the levels about 4.5 times of Dittus–Boelter levels [14] are requested.

3.3. Thermo-hydraulic performance

Fig. 5 shows the comparison of thermal performances of present scale-roughened channel with rib-roughened channels [1–6]. The thermal performance in terms of $(\overline{Nu}/Nu_\infty)/(f/f_\infty)^{1/3}$ is derived based on the same pumping power consumption [15]. As shown in Fig. 5, the decrease of thermal performance with increasing Reynolds number appears to be a common trend for rib-roughened channels with laminar and turbulent flows. In this respect, the thermal performance improved by surface ribs is deteriorated for the applications involving high Reynolds numbers such as the cooling of gas turbine blade. However, the thermal performances in scaled-roughened channels with forward and downward turbulent flows are steadily remained when

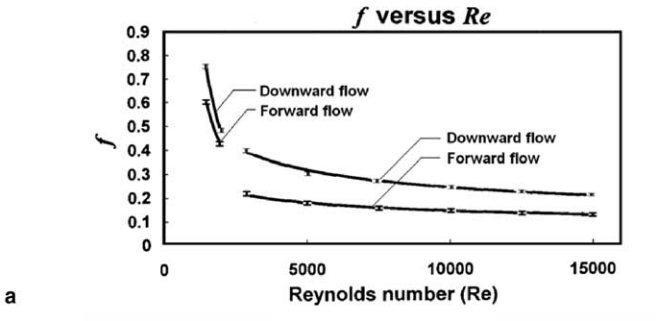

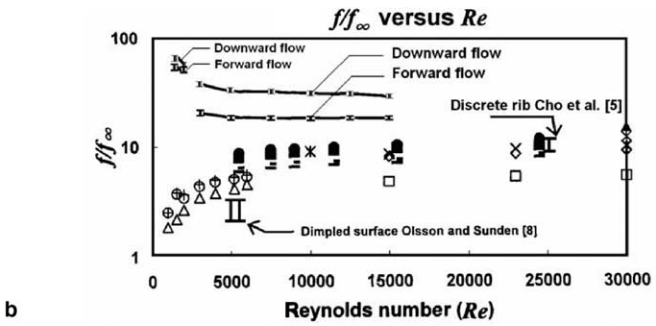

Symbols	References	Channel aspect ratio	Rib attack angle	P/e	e/H	Type of roughness
	Forward flow (present study)	8		10	0.1	Scaled surface
	Downward flow (present study)	8		10	0.1	Scaled surface
	Taslim et al. 45deg V-Up [1]	1	45	10	0.083	Continuous rib
	Taslim et al. 45deg V-Down [1]	1	45	10	0.083	Continuous rib
	Taslim et al. 45deg [1]	1	45	10	0.083	Continuous rib
	Taslim et al. V Discrete [1]	1	45	10	0.083	Discrete rib
	Han et al. 45deg V-Up [2]	1	45	10	0.0625	Continuous rib
	Han et al. 45deg V-Down [2]	1	45	10	0.0625	Continuous rib
	Han et al. 45deg [2]	1	45	10	0.0625	Continuous rib
	Gao & Sunden 60deg V-Up [3]	8	60	10	0.1	Continuous rib
	Gao & Sunden 60deg V-Down [3]	8	60	10	0.1	Continuous rib
	Gao & Sunden 60deg [3]	8	60	10	0.1	Continuous rib
	Han & Park 60deg (developing) [6]	4	60	10	0.125	Continuous rib
	Park et al. 45deg Parallel [4]	4	45	10	0.125	Continuous rib
	Cho et al. [5]	2	45	10	0.1	Discrete rib
	Olsson & Sunden [8]	7.6、14		10.6	0.27	Dimpled surface

Fig. 4. Comparison of friction performance in scale-roughened channel with dimpled and scale-roughened channels.

the Reynolds number increases. This data trend found in the scaled-roughened channel is attributed from the steady performance of heat transfer augmentation in the turbulent flow regime as demonstrated in Fig. 3. For laminar flows, the thermal performances in present scale-roughened channel increase with increasing Reynolds number, which trend reverses the typical results found in rib-roughened channels [3]. Justified by the data trends depicted in Fig. 5, the scale-roughened channel with forward flows could offer better thermal performances than the rib-roughened channels at high Reynolds numbers above than 10,000.

It is worth mentioning that the thermal performances in rib-roughened narrow channels [3] are consistently lower than those counterparts in the square channels [1,2] even if the ribbing geometries in these rib-roughened channels are similar. The levels of thermal performance with forward turbulent flows in present scale-roughened narrow channel are comparable with a variety of square-sectioned rib-roughened channels [1,2] and much higher than the rib-roughened narrow channels with the same width-to-height ratio of 8 [3]. Nevertheless, the thermal performances in scale-roughened channel with downward flows are the lowest ones

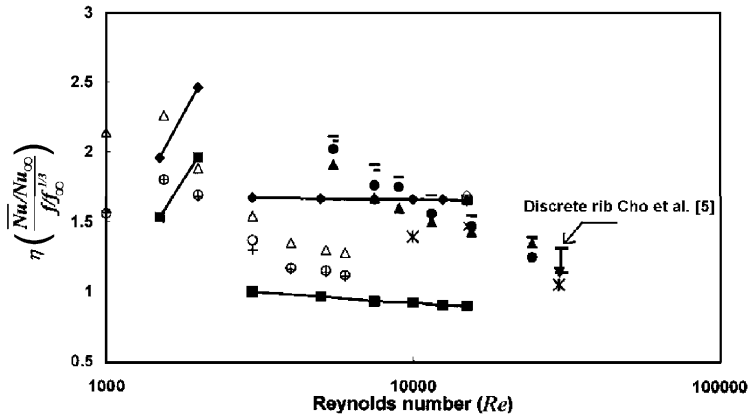

Symbols	References	Channel aspect ratio	Rib attack angle	P/e	e/H	Type of roughness
	Forward flow (present study)	8		10	0.1	Scaled surface
	Downward flow (present study)	8		10	0.1	Scaled surface
▲	Taslim et al. 45deg V-Up [1]	1	45	10	0.083	Continuous rib
●	Taslim et al. 45deg V-Down [1]	1	45	10	0.083	Continuous rib
—	Taslim et al. 45deg [1]	1	45	10	0.083	Continuous rib
-	Taslim et al. V Discrete [1]	1	45	10	0.083	Discrete rib
◇	Han et al. 45deg V-Up [2]	1	45	10	0.0625	Continuous rib
×	Han et al. 45deg V-Down [2]	1	45	10	0.0625	Continuous rib
□	Han et al. 45deg [2]	1	45	10	0.0625	Continuous rib
+	Gao & Sunden 60deg V-Up [3]	8	60	10	0.1	Continuous rib
△	Gao & Sunden 60deg V-Down [3]	8	60	10	0.1	Continuous rib
○	Gao & Sunden 60deg [3]	8	60	10	0.1	Continuous rib
▼	Han & Park 60deg (developing) [6]	4	60	10	0.125	Continuous rib
✱	Park et al. 45deg Parallel [4]	4	45	10	0.125	Continuous rib
⊥	Cho et al. [5]	2	45	10	0.1	Discrete rib

Fig. 5. Comparison of thermal performances between scaled-roughened and rib-roughened channels.

due to the high friction losses as seen in Fig. 5. Recalling the heat transfer performances compared in Fig. 3 for scale-roughened and rib-roughened channels, the present scale-roughened channel with forward flow could offer the highest values of heat transfer augmentation with the similar levels of thermal performance, which are suitable for applications with high Reynolds numbers.

4. Conclusions

This experimental study examined the heat transfer and pressure drop in a scale-roughened narrow channel with width-to-height ratio of 8. The streamwise heat transfer data along with the friction factors of the scale-roughened channel with forward and downward flows at eight different Reynolds numbers in the range of $1500 \leqslant Re \leqslant 15{,}000$ were acquired and the empirical correlations for Nu and f generated. Due to the subtle differences in the flow structures between forward and downward flows in the present scale-roughened channel, the Nusselt number ratios (Nu/Nu_∞) for laminar forward and downward flows were in the range of 7.4–9.2 and 6.2–7.4 respectively. The values of Nu/Nu_∞ for turbulent developed flows in the scale-roughened narrow channel with forward and downward flows were about 4.5 and 3 respectively. The friction factors in the scale-roughened channel with forward flows were consistently lower than those downward-flow counterparts, which were considerable higher than the values in rib-roughened channels. The better thermal performances of scale-roughened channel with forward flow relative to the comparative groups of rib-roughened channels could be developed at high Reynolds numbers of $Re > 10{,}000$. The present scale-roughened channel with forward flow could offer the highest levels of heat transfer augmentation having similar values of thermal performance factors with the comparative rib-roughened channels, which are suitable for high Reynolds number applications. A detailed study aimed at applying this scale-

roughened surface to rotating and reciprocating surfaces is worthwhile for the cooling applications of gas turbine rotor blade and piston.

References

[1] M.E. Taslim, T. Li, D. Kercher, Experimental heat transfer and friction in channels roughened with angle, V-shaped, and discrete ribs on two opposite walls, ASME J. Turbomachinery 118 (1996) 20–28.

[2] J.C. Han, Y.M. Zhang, C.P. Lee, Augmented heat transfer in square channels with parallel, crossed, and V-shaped angled ribs, ASME J. Turbomachinery 113 (1991) 590–597.

[3] X. Gao, B. Sunden, Heat transfer and pressure drop measurements in rib-roughened rectangular ducts, Exp. Therm. Fluid Sci. 24 (2001) 25–34.

[4] J.S. Park, J.C. Han, Y. Huang, S. Ou, R.J. Boyle, Heat transfer performance comparisons of five different rectangular channels with parallel angled ribs, Int. J. Heat Mass Transfer 35 (1992) 2891–2903.

[5] H.H. Cho, S.J. Wu, H.J. Kwon, Local heat/mass transfer measurement in a rectangular duct with discrete ribs, ASME J. Turbomachinery 122 (2000) 579–586.

[6] J.C. Han, J.S. Park, Developing heat transfer in rectangular channels with rib turbulators, Int. J. Heat Mass Transfer 31 (1988) 183–195.

[7] G.I. Mahmood, M.L. Hill, D.L. Nelson, P.M. Ligrani, H.-K. Moon, B. Glezer, Local heat transfer and flow structure on and above a dimpled surface in channel, ASME J. Turbomachinery 123 (2001) 115–123.

[8] C.-O. Olsson, B. Sunden, Heat transfer and pressure drop characteristics of 10 radiator tubes, Int. J. Heat Mass Transfer 39 (1996) 3211–3220.

[9] St. Tiggelbeck, N.K. Mitra, M. Fiebig, Experimental investigations of heat transfer enhancement and flow losses in a channel with double rows of longitudinal vortex generators, Int. J. Heat Mass Transfer 36 (1993) 2327–2337.

[10] J.X. Zhu, M. Fiebig, N.K. Mitra, Numerical investigation of turbulent flows and heat transfer in a rib-roughened channel with longitudinal vortex generators, Int. J. Heat Mass Transfer 38 (1995) 495–501.

[11] X. Gao, B. Sunden, PIV measurement of the flow field in rectangular ducts with 60° parallel, crossed and V-shaped ribs, Exp. Therm. Fluid Sci. 28 (2004) 639–653.

[12] S.W. Chang, K.F. Chiang, T.L. Yang, P.H. Chen, Heat transfer in a twin-blow narrow channel with two opposite walls roughened by skewed ribs arranged in staggered manner, Int. J. Therm. Sci. 44 (2005) 694–708.

[13] JHT Editorial Board of ASME J. Heat TransferJ. Heat Transfer Policy on Report Uncertainties in Experimental Measurements and Results, ASME J. Heat Transfer 115 (1993) 5–6.

[14] F.W. Dittus, L.M.K. BoelterPublications in Engineering, vol. 2, University of California, Berkeley, CA, 1930, p. 443.

[15] D.L. Gee, R.L. Webb, Forced convection heat transfer in helically rib-roughened tubes, Int. J. Heat Mass Transfer 23 (1980) 1127–1136.